

Novel experimental approach for longitudinal-radial stiffness characterisation of clear wood by a single test

José Xavier^{1,2,*}, Stéphane Avril¹, Fabrice Pierron¹ and José Morais²

¹ LMPF/ENSAM, Châlons-en-Champagne Cedex, France

² CETAV/UTAD, Vila Real, Portugal

*Corresponding author.

LMPF/ENSAM, Rue Saint-Dominique BP 508,
51006 Châlons-en-Champagne Cedex, France
E-mail: jose.xavier@chalons.ensam.fr

Abstract

Experimental results obtained from maritime pine (*Pinus pinaster* Ait.) wood are presented for the characterisation of all LR=(1,2) orthotropic stiffness parameters of clear wood specimens by a single test. The approach relies on application of the virtual field method (VFM) to a rectangular specimen loaded in the Iosipescu fixture. The displacement field over the gauge surface of the specimen is measured by the grid method. Two configurations are investigated: (1) with grain aligned along the specimen length (0° configuration) and (2) with grain at 45°. For the 0° configuration, only the parameters Q_{11} and Q_{66} are correctly identified, with coefficients of variation of the same order of magnitude as those obtained from reference tensile and shear tests. Better identification is obtained for the 45° configuration, for which only the parameter Q_{12} exhibits large scatter. This improvement results from a more balanced influence of all stiffness parameters on the response of the 45° specimen. However, all stiffness parameters identified were systematically underestimated by approximately 30% in comparison to reference values. This deviation is due to the vertical spatial variation of the mechanical properties of wood within the stem. Literature data confirm this interpretation.

Keywords: full-field measurements; material characterisation; statically undetermined test; virtual fields method (VFM).

Introduction

To describe the complex behaviour of wood based on given parameters is difficult, and correct experimental characterisation of the parameters governing a constitutive law is particularly challenging. This is the case even when clear wood is modelled as a continuous and homogeneous material, with orthotropic linear elastic behaviour along the longitudinal (L,1), radial (R,2) and tangential (T,3) directions of the wood cells (Guitard 1987; Smith et al. 2003). Conventionally, the material parameters describing this behaviour are experimentally determined by carrying out several statically determined tests (e.g.,

tensile, compression, bending and shear tests) on specimens with simple geometries (e.g., rectangular), oriented along the material symmetry axes and containing a few annual rings (ASTM D143 1994). This approach involves considerable effort for accurate characterisation of wood mechanical properties because of the inherent anisotropy and variability of wood.

Digitisation combined with full-field optical techniques (FFOTs) yields new methods for material characterisation of a given surface (Grédiac 2004): (1) digital image correlation (Rastogi 2000); (2) moiré interferometry (Post et al. 1994); (3) speckle interferometry (Cloud 1995); (4) shearography (Hung and Ho 2005); and (5) grid methods (Surrel 2004). A specimen with appropriate geometry can be loaded in such a way that several parameters are simultaneously involved in its mechanical response. From the kinematic fields measured by FFOTs, all these active parameters may be determined in a single test using a suitable identification strategy. This seems particularly interesting for the characterisation of wood properties due to its anisotropy and variability.

Data processing by finite element model updating (FEMU) (Le Magorou et al. 2002) or the virtual field method (VFM) (Grédiac et al., 2006) is suitable for deriving material properties from full-field measurements.

Only the VFM approach is considered in this study of the linear elastic orthotropic behaviour of maritime pine wood (*Pinus pinaster* Ait.) in the LR=1,2 plane of symmetry. It is straightforward and simple. A macroscopic homogeneous model of the material is considered:

$$\begin{Bmatrix} \sigma_1 \\ \sigma_2 \\ \sigma_6 \end{Bmatrix} = \begin{bmatrix} Q_{11} & Q_{12} & 0 \\ Q_{12} & Q_{22} & 0 \\ 0 & 0 & Q_{66} \end{bmatrix} \begin{Bmatrix} \varepsilon_1 \\ \varepsilon_2 \\ \varepsilon_6 \end{Bmatrix}, \quad (1)$$

where σ_i is the stress field vector, ε_i is the strain field vector and Q_{11} , Q_{22} , Q_{12} and Q_{66} are the stiffness parameters to be determined experimentally. The objective of this paper is to investigate the ability of VFM to simultaneously identify the four LR stiffness parameters in a wooden rectangular specimen loaded in the Iosipescu fixture.

Wood appears as heterogeneous on the scale of our study due to latewood (LW) and earlywood (EW) layers within the growth rings (Figure 1). However, it has been verified by Xavier et al. (2005) that the size of the specimen and the size of the annual rings are suitable to obtain “homogenised” properties of clear wood using the present approach. In the quoted work, a finite element model of layered material with different properties in LW and EW phases was applied and displacement fields were simulated. The results were in very good agreement with the homogenised properties according to the law of

mixtures of the layered material. Thus, in the present paper, the material was supposed to be homogeneous.

Materials and methods

Tree and specimens

The material used was manufactured from a single *Pinus pinaster* Ait. tree of 74 years of age that was grown in the district of Viseu (Portugal). Specimens cut at approximately 8 m from the basal plane of the tree were available. These sawn and planed boards were dried in a kiln to a moisture content of 10–12% before cutting the specimens from the outer part.

The specimens consisted of beams of $80 \times 20 \times 5$ mm³ cut in the LR plane of symmetry. A total of 14 specimens were investigated here, seven with grain orientation at a nominal angle of 0° with regard to the longitudinal axis of the specimen, and seven with grain orientation of 45° (Figure 1a). The average width of the growth rings was approximately 2 mm. The equilibrium state of humidity was reached before testing. The oven-dry density of the specimens (determined as the ratio between the oven-dry weight and green volume) was found to be between 0.505 and 0.559 g cm⁻³. Using the oven-dry method, the moisture content of the specimens during testing was determined to be approximately 9–10%.

Full-field measurements

The grid method chosen in this study has better spatial resolution than digital image correlation, for instance. It is applicable to all types of materials and is less sensitive to vibrations than interferometric techniques. It provides measurement of the in-

plane displacement field by studying the deformation of a grid. The grid consists of a periodic pattern of white and black contrasting lines and is assumed to be perfectly bound to the specimen. A detailed description of the grid method can be found in Surrel (2004).

A grid with a pitch (p) of 0.1 mm, i.e., 10 lines mm⁻¹, was employed here, covering a field of view of 34×20 mm² ($L \times W$ in Figure 1c) at the centre of the specimen. It was imaged using a PCO SenSicam CCD camera of 1376×1040 pixels with a pixel size (on the object plane) of 0.025 mm, i.e., approximately 4 pixels per period (Figure 1c). The grid was transferred according to the procedure described by Piro and Grédiac (2004).

Images of the grid in the deformed and undeformed states were analysed using a phase shifting approach (Dorrio and Fernández 1999; Surrel 1999). The windowed DFT algorithm was used in this work because of its ability to eliminate some of the systematic errors inherent to grid images (Surrel 1996, 1999). It provides two phase fields. The difference between these phase fields is linearly tied to the displacement field:

$$u_{\beta}(x,y) = -\frac{p}{2\pi} \Delta \phi_{\beta}(x,y), \quad (2)$$

where $\beta = x$ and y , respectively for the horizontal (from a grid with vertical lines) and vertical (from a grid with horizontal lines) components of the displacement. In our experiments, the displacement resolution, i.e., the smallest displacement value that can be detected or measured, lies between 0.9 and 1.2 μ m. The spatial resolution required to achieve this accuracy is 1 period (distance between two contiguous lines) here, i.e., 0.1 mm.

The in-plane strain fields required for identification of the material parameters were determined using a polynomial approximation of the raw data provided by the grid method,

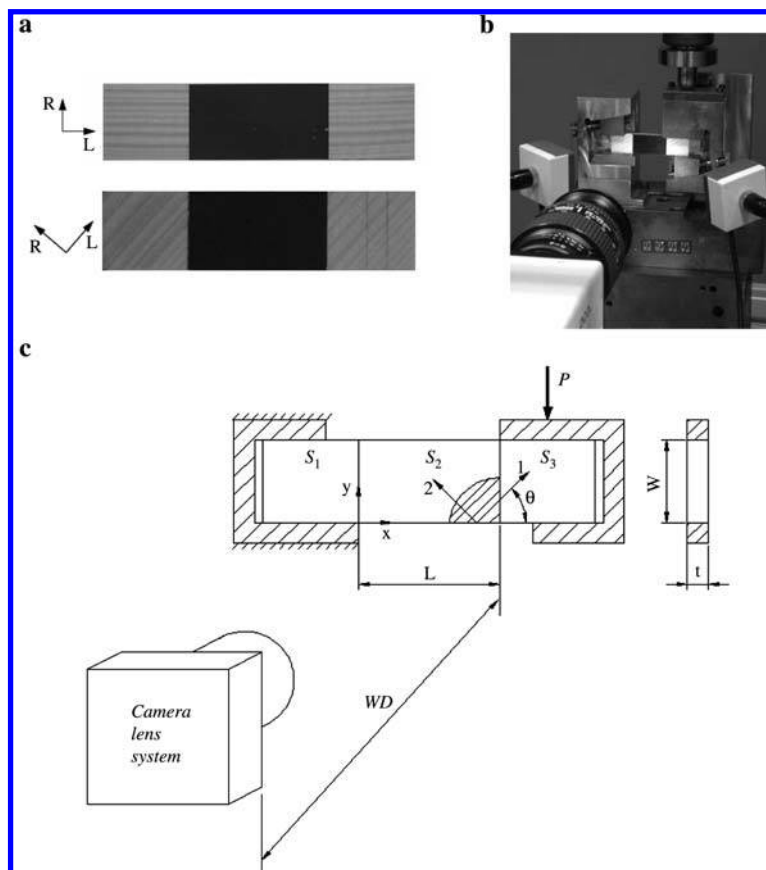


Figure 1 Images of (a) the 0° and 45° specimens and (b) the mechanical set-up. (c) Sketch of the mechanical set-up (WD, working distance, approx. 450 mm).

followed by numerical differentiation (Pannier et al. 2006). This approach is particularly suitable when the frequencies of the signal (low) and noise (high) are well separated, which was assumed here.

Shear/bending mechanical test

A specific shear/bending mechanical test was designed that involves the stiffness parameters Q_{11} , Q_{22} , Q_{12} , and Q_{66} in the deformation of a single specimen (Pierron and Grédiac 2000; Grédiac et al. 2002b; Chahar et al. 2006). It consists of loading a straight rectangular beam with the Iosipescu fixture (Figure 1c). The V-notches of the classical geometry of the Iosipescu specimen (ASTM D5379 1993) are removed here. The length between the inner supports (L) and the grain angle (θ) are adjusted to maximise the identifiability of the stiffness properties by the VFM (Avril et al. 2004b).

Experimentally, the load was applied at a controlled displacement rate of 1 mm min^{-1} and measured with a 100-kN load cell. Before the tests, specimens were loaded and unloaded five times up to a load of approximately 50 N to improve the flatness and parallelism of their loading surfaces. Because only the linear elastic mechanical response of the specimens was investigated here, the tests were stopped when a load of approximately 200 N was reached. This load range was found to be adequate for stiffness identification.

Stiffness parameter identification by VFM

The problem to be solved here is the simultaneous identification of Q_{11} , Q_{22} , Q_{12} , and Q_{66} from measurements of the resultant load, the strain fields and specimen geometric parameters. VFM (Grédiac et al. 2006) is an identification procedure suitable for solving this type of inverse problem. It is based on two fundamental equations in solid mechanics: the static equilibrium equation – the principle of virtual work (PVW) – and the constitutive stress-strain equation. In a first step, the method consists of replacing the constitutive equation [Eq. (1)] into the PVW, which yields, by assuming a plane stress problem and the absence of body forces, the following equation:

$$Q_{ij} \int_S \varepsilon_i \varepsilon_j^* dS = \frac{1}{t} \int_{S_t} T_i(M, n_\beta) \cdot u_\beta^*(M) dS, \quad (3)$$

where ε_i^* is the virtual strain field, u_β^* is the virtual displacement field, S is the surface for which measurements are available, t is the thickness of the plate, and $T_i(M, n_\beta)$ is the distribution of external tractions applied over the boundary S_t (M is any point on this surface and n_β is the outward normal vector at point M).

Rewriting Eq. (3) with as many different virtual fields (u_β^* , ε_i^*) as there are unknown parameters yields a linear system of equations. The virtual fields are actually special virtual fields, i.e., satisfying some specific conditions (Grédiac et al. 2002a,b). Moreover, they are expanded here using piecewise bilinear test functions (Toussaint et al. 2006). Finally, they are determined as the solution of a constrained optimisation problem (Avril et al. 2004a). This ensures that the solution obtained is less sensitive to experimental noise.

Results and discussion

Flowchart of the procedure

The image processing and identification procedures were performed using Matlab® functions (developed in house) according to the flowchart presented in Figure 2.

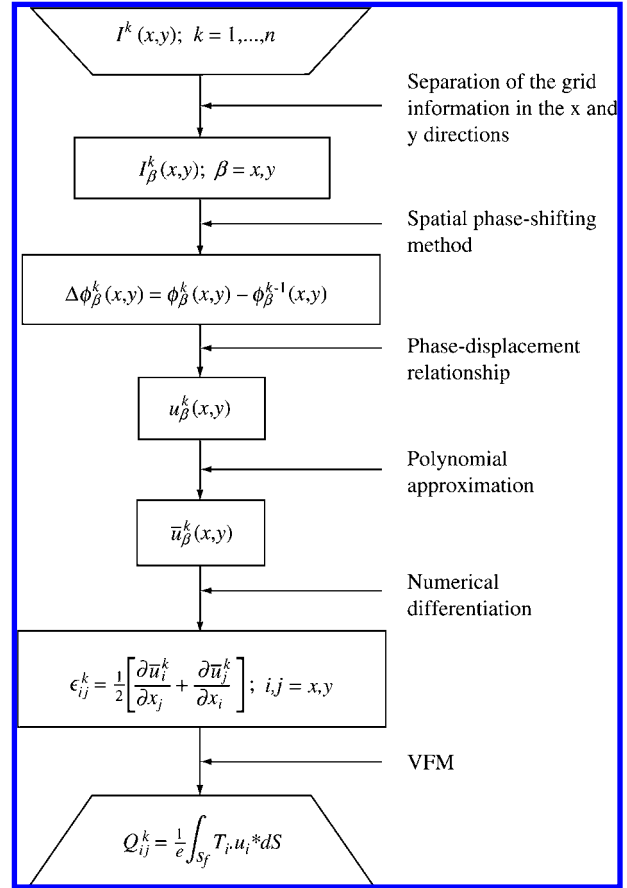


Figure 2 Flowchart of the image processing and identification procedures.

0° specimen

Throughout the data processing, several parameters have to be carefully selected because they may significantly affect the final results. In particular, choice of the polynomial degree for the approximation of raw displacement data is crucial. Thus, we identified stiffness parameters using different polynomial degrees. Results are presented in Figure 3 for a 0° specimen. For each polynomial degree, the parameters were determined from 27 load values from 73 to 140 N. It is evident in Figure 3 that the scattering bars are quite large for degrees greater than 7. For degrees less than 7, noise minimisation is more efficient and the results are uniform. However, the polynomials are unable to accurately fit the actual fields and this induces a bias in the results by overestimation of Q_{11} and Q_{12} . This bias was also observed by processing simulated data provided by a finite element code. Therefore, degree 7 is a good compromise between noise minimisation and good fitting and was retained for the whole study. An example of the measured and approximated displacement fields, along with their difference, is presented in Figure 4 for a 0° specimen. The difference fields have low-intensity random values, indicating that some noise has been subtracted from the original displacement fields during the fitting process.

Derived strain fields are displayed in Figure 5a. It is evident that the ε_6 field component (Figure 5a.3) is predominant over those derived from the other two components. The strain fields (Figure 5a) were compared with

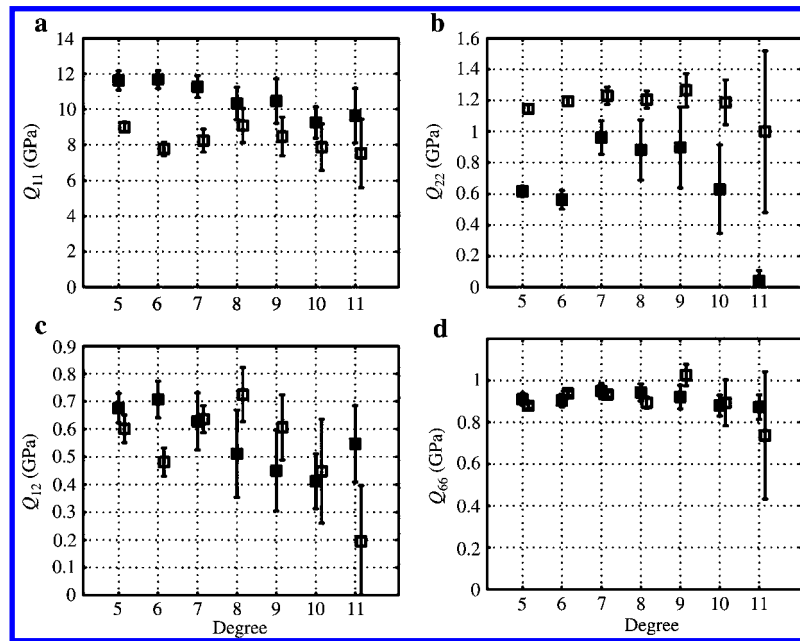


Figure 3 Variation of the stiffness parameters with respect to the degree of the fitting polynomial for 0° (■) and 45° (□) specimens: (a) Q_{11} , (b) Q_{22} , (c) Q_{12} , and (d) Q_{66} .

numerical values (Figure 5b) computed using a finite element model with the ANSYS 8.0® package. Wood was modelled as a continuous, homogeneous and orthotropic material with the elastic properties identified by VFM in the experiments. Despite a reasonable match between experimental and numerical fields, it is interesting to note the significant differences near the borders of the region

of interest. These differences reveal that the polynomial fitting approach used here may induce some systematic errors in the strain computation in these areas. Nevertheless, these errors only slightly affect the VFM process (Grédiac et al. 2006).

Typical results obtained with the VFM are presented in Figure 6, in which the stiffness parameters are plotted

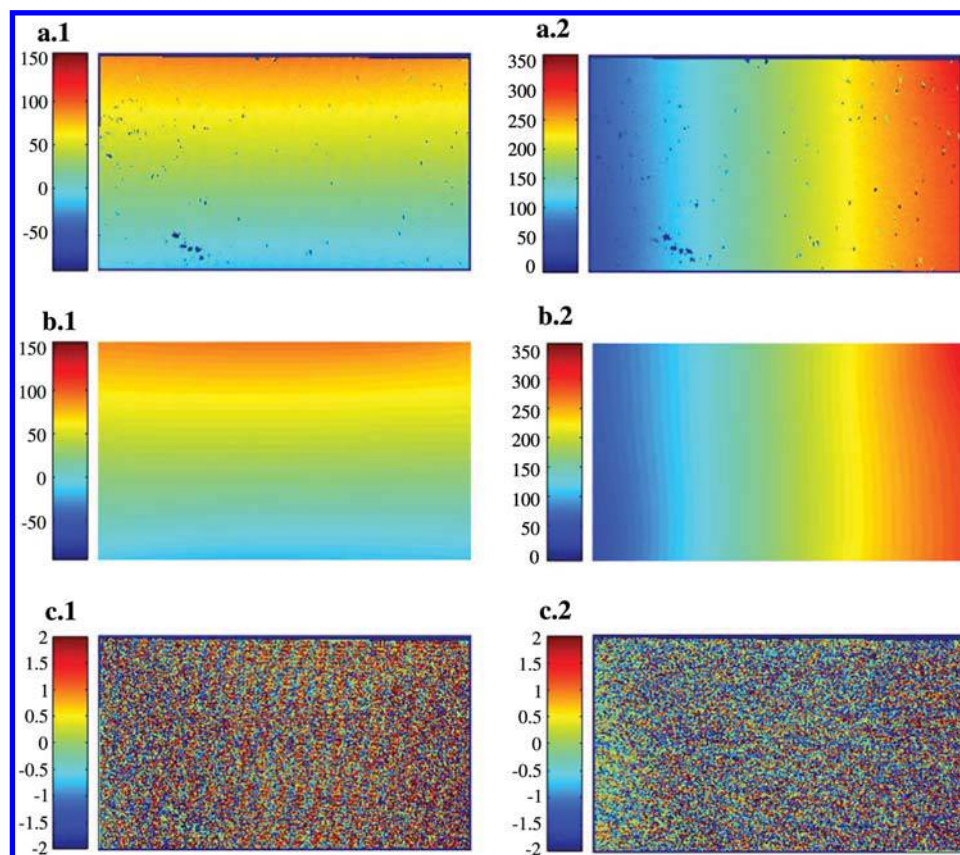


Figure 4 (a) Measured, (b) approximated and (c) residual (1) x and (2) y displacement fields obtained for a 0° specimen (μm).

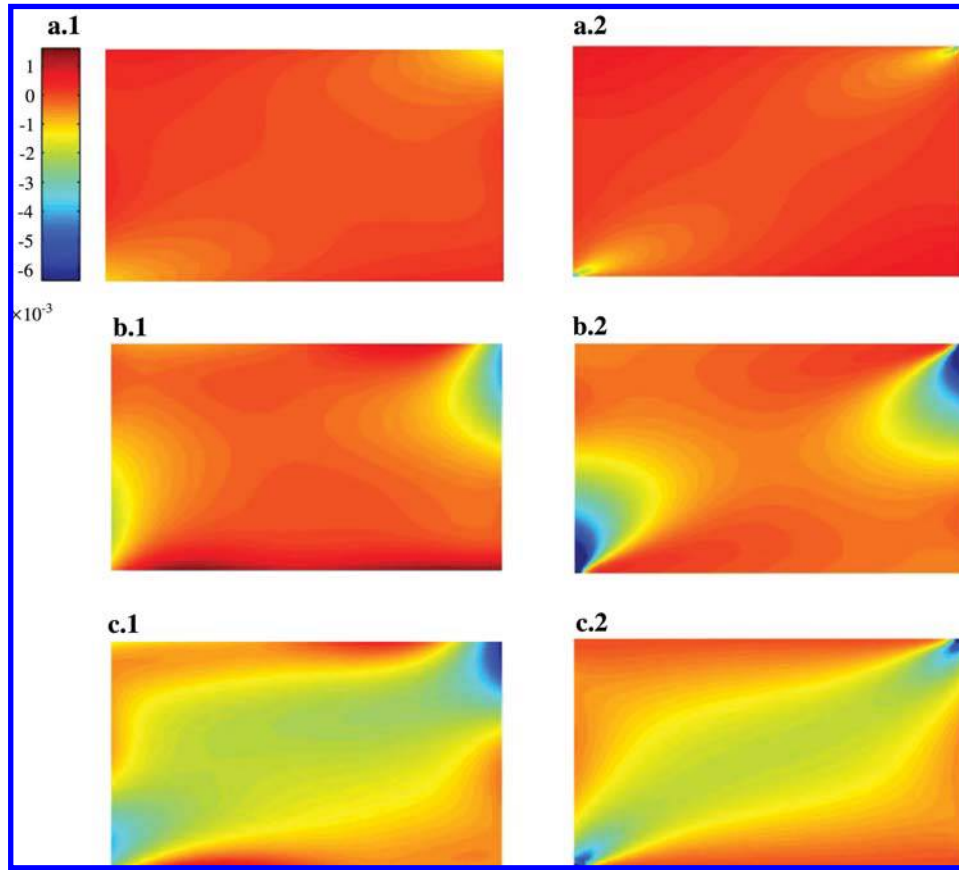


Figure 5 Typical (1) experimental and (2) simulated strain fields for the 0° specimen ($P = -139.4$ N): (a) ε_1 , (b) ε_2 , and (c) ε_6 .

versus the applied load. It can be observed that the data conveniently converge to a mean value for both Q_{11} and Q_{66} . However, all along the load interval, scattered data are obtained for both Q_{22} and Q_{12} , which compromises their convergence to an identifiable value. This result may be perceived as a first indication that the 0° configuration may be not suitable for correct identification of these two last parameters.

An applied load interval was chosen for evaluating an average value for each stiffness parameter. It was selected individually for each specimen to eliminate aberrant results. The criterion is to exclude applied loads that are

“too low” for which the signal-to-noise ratio is still low and the loads that are “too high” for which the non-linear response of the material may have been already reached. For instance, in Figure 6 the applied load interval was in the range from 73 to 140 N. In other words, this interval is selected to reduce the standard deviation associated with the mean stiffness values determined among the specific applied load range.

The average values of Q_{11} , Q_{22} , Q_{12} , and Q_{66} identified by VFM in these intervals for the 0° specimens, along with the specimen density (ρ), are summarised in Table 1. After checking the normality of the distributions of the

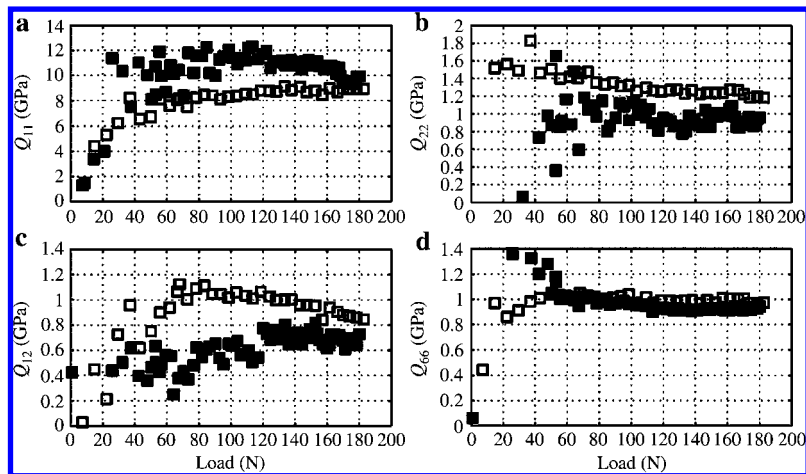


Figure 6 Identified stiffness parameters plotted versus the applied load for 0° (■) and 45° (□) specimens: (a) Q_{11} , (b) Q_{22} , (c) Q_{12} , and (d) Q_{66} .

Table 1 Oven-dry densities and stiffness properties of *Pinus pinaster* Ait. wood identified by the virtual field method (VFM) using 0° specimens.

Specimen	ρ (g cm ⁻³)	Q_{11} (GPa)	Q_{22} (GPa)	Q_{12} (GPa)	Q_{66} (GPa)
1	0.508	10.0	0.916	0.351	0.777
2	0.505	11.0	1.03	0.589	0.985
3	0.522	9.73	0.763	0.551	0.835
4	0.509	10.3	0.303	0.294	0.992
5	0.531	10.3	0.605	0.558	0.948
6	0.537	10.5	0.256	0.335	1.07
7	0.534	10.1	0.417	0.209	0.963
Mean	0.521	10.26	0.613	0.412	0.939
95% CI		±0.388	±0.280	±0.138	±0.092
CV (%)	2.6	4.09	49.4	36.9	10.6
Reference		15.6	1.97	0.926	1.41
Difference (%)		34	69	55	33

CI, confidence intervals. CV, coefficient of variation.

stiffness values by the Shapiro-Wilk test (Neuilly 1999), the 95% confidence intervals for the mean of each parameter were determined from the t-distribution (Table 1). It can be concluded from these results that Q_{22} and Q_{12} are identified with very large scatter, confirming that the 0° configuration is not suitable for their accurate identification. Similar results were also obtained for a unidirectional glass/epoxy composite material (Chalal et al. 2006). This result may be understood from the ε_2 strain field. In fact, the Q_{22} and Q_{12} parameters are directly proportional to ε_2 , and it was noted that the intensity of this strain component is significant only in concentrated zones near the inner supports (Figure 5b). Hence, the identifiability of these parameters is lower. This can also be analysed in terms of sensitivity to noise, which is higher for Q_{22} and Q_{12} than for Q_{11} and Q_{66} for the 0° specimen (Pierron et al. 2006). This is confirmed by the low scatter associated with the Q_{11} and Q_{66} parameters (Table 1).

The results obtained with VFM for Q_{11} and Q_{66} were compared with “reference” stiffness values for *P. pinaster* wood reported in Table 2. These reference parameters were determined experimentally from tensile tests along the longitudinal and radial directions (Pereira 2005), and a classical Iosipescu shear test (Xavier et al. 2004). The specimens for these reference tests were taken from the same tree as for the experiments presented in this paper, but from a lower position of 6 m approximately. Accordingly, the specimens for the tests of this paper and references did not match perfectly. Nonetheless, these references are reported here in order to comment on our results.

It is evident that a close Q_{11}/Q_{66} anisotropic ratio is obtained between the present results (10.9) and the references (11.0). These ratios are also in agreement with

those deduced for loblolly pine wood ($Q_{11}/Q_{66} = 12.3$; Forest Products Laboratory 1999). However, the average values of Q_{11} and Q_{66} are lower than those of the references by 34% and 33%, respectively. We interpret the underestimation of both Q_{11} and Q_{66} as a result of vertical spatial variation of the wood mechanical properties within the stem. A recent study (Machado and Cruz 2005) has shown that a decrease of approximately 29–35% (depending on the radial position of the specimens) of the longitudinal modulus (E_L) can be found for specimens cut at different heights within the stem (separated by approx. 60% of the whole height of the tree). Machado and Cruz (2005) explained this vertical decrease in E_L in terms of the greater percentage of juvenile wood at higher positions within the stem, which leads to lower density (Louzada 2000). The same phenomenon is observed here: the mean density reported in Table 1 is lower compared to that of the references (Table 2). However, the density variation alone cannot explain the stiffness differences obtained here, at least if we assume a linear relationship between density and stiffness (Gibson and Ashby 1997). Other morphological differences, such as the microfibril angle, may also contribute to the differences observed for mean values of the stiffness parameters measured in this work and those for the references (Barnett and Bonham 2004).

45° specimen

Specimens with the grain rotated by 45° with regard to its longitudinal axis were tested (Figure 1a). The same procedure as described above was applied.

The stiffness parameters identified with different degrees of polynomials are presented in Figure 3. It is

Table 2 Reference stiffness values of *Pinus pinaster* Ait. wood identified through standard tests (Pereira 2005; Xavier et al. 2004).

	(L) tensile test			(R) tensile test		(LR) Iosipescu test	
	ρ (g cm ⁻³)	Q_{11} (GPa)	Q_{12} (GPa)	ρ (g cm ⁻³)	Q_{22} (GPa)	ρ (g cm ⁻³)	Q_{66} (GPa)
Mean	0.616	15.54	0.92	0.697	1.97	0.589	1.41
95% CI		±0.580	±0.055		±0.089		±0.112
CV (%)	2.0	7.1	7.3	0.9	7.9	5.6	10.3

CI, confidence intervals. CV, coefficient of variation.

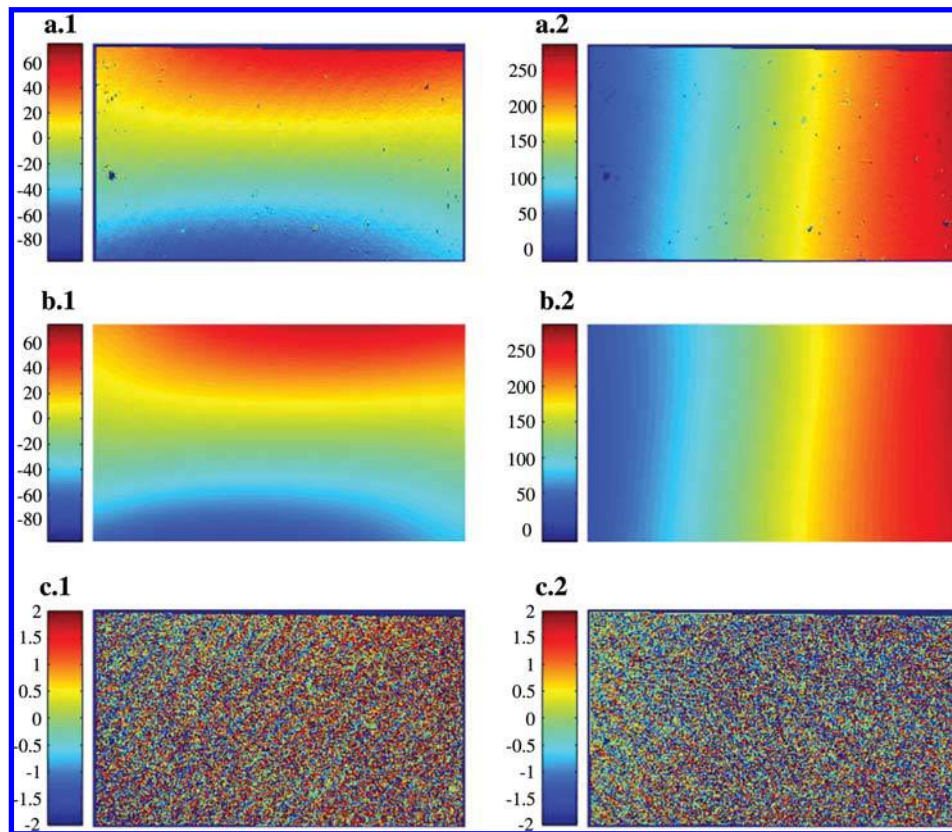


Figure 7 (a) Measured, (b) approximated and (c) residual (1) x and (2) y displacement fields obtained for a 45° specimen (μm).

evident that: (1) the stiffness parameters tend to decrease for higher degrees; and (2) scattering for the stiffness values increases with increasing degree. Hence, a degree of 7 was chosen as a compromise between accuracy and stability, as for the 0° specimens. An example of measured and approximated displacement fields is illustrated in Figure 7. The conclusion regarding the filtering effect of the polynomial approximation is the same as for the 0° specimens.

The derived strain fields computed in the (1,2) material reference axes are shown in Figure 8a. It can be pointed out here that both the ε_1 and ε_2 fields are more evenly spread over the region of interest than for the 0° specimen. Thus, rotation of the specimen grain clearly yields a more balanced distribution of strains over the region of measurements. Thus, better identification of the four stiffness components can be expected.

Comparison of the experimental strain fields (Figure 8a) with the equivalent values modelled by finite element analysis (Figure 8b) reveals only some marginal differences. These are located near the edges and are induced by the polynomials. In Figure 6, an example of the variation of the stiffness parameters versus the applied load is plotted. Good convergence towards the average value (without a high degree of scattering) is reached for the Q_{11} , Q_{22} , and Q_{66} parameters with increasing load. Identification of Q_{12} remains low. This result is not unexpected because this parameter involves Poisson's effect, which is usually small and therefore more difficult to measure.

The average LR stiffness parameters and density of *P. pinaster* wood identified by VFM from the shear/bending test are summarised in Table 3. The 95% confidence

intervals for the mean stiffness parameters were determined from the t-distribution after checking for normality by the Shapiro-Wilk test (Table 3). For this configuration, both the Q_{22} and Q_{66} parameters are identified with scatter of the same order of magnitude as for the reference tests. However, greater dispersion is obtained for Q_{11} and Q_{12} , which are still highly scattered. Because of identifiability reasons, only Q_{11} and Q_{66} stiffness values are comparable for the 0° (Table 1) and 45° (Table 3) specimens: almost the same mean values were found. This is statistically confirmed by a t-test for equality of the means at a 95% confidence level.

For the VFM results, the anisotropic ratios were similar for the specimens and references for Q_{11}/Q_{22} (8.2 and 7.9) and Q_{11}/Q_{66} (10.7 and 11.0, respectively). These ratios are also in agreement with those deduced from reference properties reported for similar species (loblolly pine, $Q_{11}/Q_{22}=8.8$ and $Q_{11}/Q_{66}=12.3$; Forest Products Laboratory 1999). Nevertheless, when comparing absolute values, lower estimations are again noted for the 45° specimens of the order of 35%, 37%, 29% and 33%, respectively, for Q_{11} , Q_{22} , Q_{12} , and Q_{66} (Tables 2 and 3). As previously stated, the vertical spatial variation of the mechanical properties of wood within the stem (Machado and Cruz 2005) is believed to be the major reason for this systematic underestimation of the stiffness values.

Conclusion

The approach presented in this paper is based on VFM application to a rectangular beam loaded with the losi-

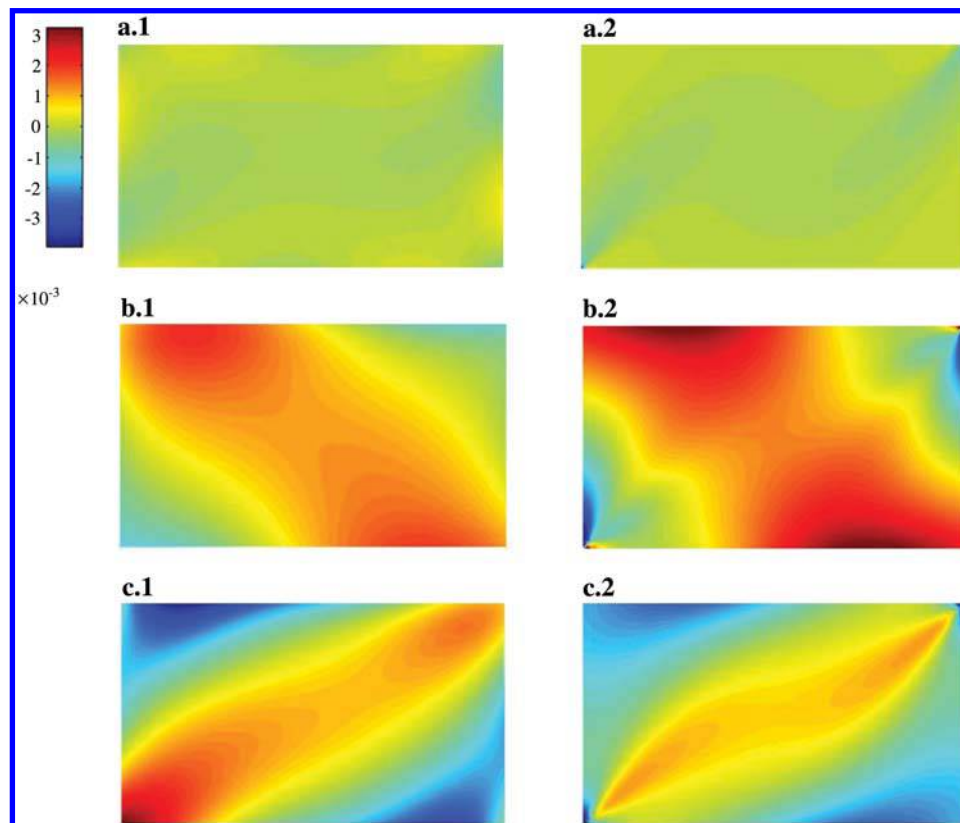


Figure 8 Typical (1) experimental and (2) simulated strain fields for the 45° specimen ($P = -142.4$ N): (a) ε_1 , (b) ε_2 , and (c) ε_6 .

Table 3 Oven-dry density and stiffness properties of *Pinus pinaster* Ait. wood identified by the virtual fields method (VFM) using 45° specimens.

Specimen	ρ (g cm ⁻³)	Q_{11} (GPa)	Q_{22} (GPa)	Q_{12} (GPa)	Q_{66} (GPa)
1	0.559	8.11	1.29	0.624	0.925
2	0.537	8.69	1.28	0.954	1.00
3	0.557	8.45	1.24	0.363	1.01
4	0.542	11.6	1.17	0.702	0.928
5	0.540	10.7	1.26	0.667	1.03
6	0.544	11.8	1.16	0.591	0.856
7	0.539	11.7	1.26	0.730	0.905
Mean	0.545	10.16	1.24	0.661	0.950
95% CI		± 1.552	± 0.048	± 0.163	± 0.059
CV (%)	1.6	16.5	4.22	26.7	6.67
Reference		15.6	1.97	0.926	1.41
Difference (%)		35	37	29	33

CI, confidence intervals. CV, coefficient of variation.

pescu fixture, providing that both strain fields and the resultant load are measured. The purpose was to identify a suitable configuration for characterisation of the LR stiffness parameters of clear wood.

From the 0° configuration, only the Q_{11} and Q_{66} parameters could be correctly identified. On the other hand, the 45° configuration brought about large improvements in the results, especially for Q_{22} . Only the identification of Q_{12} was low in the case of the 45° configuration. Accordingly, the grain rotation from 0° to 45° allowed more balanced strain fields and thus improved calculation of the stiffness parameters. A numerical study is currently under way to identify an angle between 0° and 90° that will optimise the results for all LR clear wood stiffness parameters, similarly to the study carried out for polymer matrix composites (Pierron et al. 2006).

The average values of the parameters identified were systematically lower than the reference values. Our explanation is that experimental inadequacies are probably responsible for this: the specimens and references were taken from different heights. Vertical spatial variation of the mechanical properties within the stem can be high (Machado and Cruz 2005). This supposition has to be confirmed by further tests.

Acknowledgements

We would like to thank Marcelo Oliveira for his help in specimen preparation and the Foundation for Science and Technology (FCT) for financial support of the PhD scholarship of J. Xavier.

References

- ASTM D143 (1994) Standard methods of testing small clear specimens of timber. American Society for Testing and Materials, Philadelphia, PA, USA.
- ASTM D5379 (1993) Test method for shear properties of composite materials by the V-notched beam method. American Society for Testing and Materials, Philadelphia, PA, USA.
- ▶ Avril, S., Grédiac, M., Pierron, F. (2004a) Sensitivity of the virtual fields method to noisy data. *Comput. Mech.* 34:439–452.
- Avril, S., Pierron, F., Grédiac, M. (2004b) Design of suitable testing configurations for identifying mechanical constitutive equations from full-field measurements. In: proceedings of the SEM Xth International Congress and Exposition, Costa Mesa, 7–10 June 2004.
- ▶ Barnett, J.R., Bonham, V.A. (2004) Cellulose microfibril angle in the cell wall of wood fibres. *Biol. Rev.* 79:461–472.
- ▶ Chalal, H., Avril, S., Pierron, F., Meraghni, F. (2006) Experimental identification of a nonlinear model for composites using the grid technique coupled to the virtual fields method. *Compos. A Appl. Sci.* 37:315–325.
- Cloud, G.L. *Optical Methods of Engineering Analysis*. Cambridge University Press, Cambridge, 1995.
- ▶ Dorrio, B.V., Fernández, J.L. (1999) Phase-evaluation methods in whole-field optical measurement techniques. *Meas. Sci. Technol.* 10:R33–R55.
- Forest Products Laboratory (1999) Wood Handbook – Wood as an Engineering Material. General Technical Report FPL-GTR-113. Forest products Laboratory, US Department of Agriculture, Madison, WI.
- Gibson, L.J., Ashby, M.F. (1997) *Cellular Solids: Structure and Properties*. 2nd ed. Cambridge University Press, Cambridge, 1997.
- ▶ Grédiac, M. (2004) The use of full-field measurement methods in composite material characterisation: interest and limitations. *Compos. A Appl. Sci.* 35:751–761.
- ▶ Grédiac, M., Toussaint, E., Pierron, F. (2002a) Special virtual fields for the direct determination of material parameters with the virtual fields method. 1 – Principle and definition. *Int. J. Solids Struct.* 39:2691–2705.
- ▶ Grédiac, M., Toussaint, E., Pierron, F. (2002b) Special virtual fields for the direct determination of material parameters with the virtual fields method. 2 – Application to in-plane properties. *Int. J. Solids Struct.* 39:2707–2730.
- ▶ Grédiac, M., Pierron, F., Avril, S., Toussaint, E. (2006) The virtual fields method: a review. *Strain* 42:233–253.
- Guitard, D. *Mécanique du Matériau Bois et Composites*. Collection Nabla. Cepadues Editions, Toulouse, France, 1987.
- ▶ Hung, Y.Y., Ho, H.P. (2005) Shearography: an optical measurement technique and applications. *Mater. Sci. Eng.* 49:61–87.
- ▶ Le Magorou, L., Bos, F., Rouger, F. (2002) Identification of constitutive laws for wood-based panels by means of an inverse method. *Compos. Sci. Technol.* 62:591–596.
- Louzada, J.L.P.C. (2000) *Variação Fenotípica e Genética em Características Estruturais na Madeira de Pinus pinaster Ait. O comprimento das fibras e a densidade até aos 80 anos de idade das árvores. Parâmetros genéticos na evolução juvenil-adulto das componentes da densidade da madeira. Série Didáctica, Ciências Aplicadas no. 143*. UTAD, Vila Real, Portugal.
- ▶ Machado, J.S., Cruz, H.P. (2005) Within stem variation of maritime pine timber mechanical properties. *Holz. Roh Werkst.* 63:154–159.
- Neuilly, M. *Modelling and Estimation of Measurement Errors*. Lavoisier Publishing, Paris, 1999.
- ▶ Pannier, Y., Avril, S., Rotinat, R., Pierron, F. (2006) Identification of elasto-plastic constitutive parameters from statically undetermined tests using the virtual fields method. *Exp. Mech.* 46:735–755.
- Pereira, J. (2005) *Comportamento mecânico da madeira em tracção nas direcções de simetria material*. Master's thesis, Universidade de Trás-os-Montes e Alto Douro, Vila Real, Portugal.
- ▶ Pierron, F., Grédiac, M. (2000) Identification of the through-thickness moduli of thick composites from whole-field measurements using the Iosipescu fixture: theory and simulations. *Compos. A Appl. Sci.* 31:309–318.
- Pierron, F., Vert, G., Burgette, R., Avril, S., Rotinat, R., Wisnom, M. (2006) Optimization of the unnotched Iosipescu test on composites for identification from full-field measurement. In: proceedings of the 6th International Congress on Modern Practice in Stress and Vibration Analysis, Institute of Physics & British Society for Strain Measurements, Bath, 5–7 September 2006.
- ▶ Piro, J.-L., Grédiac, M. (2004) Producing and transferring low-spatial-frequency grids for measuring displacement fields with moiré and grid methods. *Exp. Tech.* 28:23–26.
- Post, D., Han, G., Ifju, P. *High Sensitivity Moiré*. Springer Verlag, New York, 1994.
- Rastogi, P.K. (Ed.) *Photomechanics*. Springer Verlag, Berlin, 2000.
- Smith, I., Landis, E., Gong, M. *Fracture and Fatigue in Wood*. John Wiley & Sons, Chichester, 2003.
- Surrel, Y. (1996) Design of algorithms for phase measurements by the use of phase stepping. *Appl. Opt.* 35:51–60.
- Surrel, Y. (1999) Fringe analysis. In: *Photomechanics*, Ed. P.K. Rastogi. Springer Verlag, Berlin. pp. 57–104.
- Surrel, Y. (2004) La technique de la grille pour la mesure de champs de déplacements et ses applications. *Instrum. Mes. Métrol.* 4:193–216.
- ▶ Toussaint, E., Grédiac, M., Pierron, F. (2006) The virtual fields method with piecewise virtual fields. *Int. J. Mech. Sci.* 48:256–264.
- ▶ Xavier, J., Garrido, N., Oliveira, J., Morais, J., Camanho, P., Pierron, F. (2004) A comparison between the Iosipescu and off-axis shear test methods for the characterisation of *Pinus pinaster* Ait. *Compos. A Appl. Sci.* 35:827–840.
- Xavier, J., Avril, S., Pierron, F., Morais, J., Marinescu, M. (2005) Identification of clear wood orthotropic stiffnesses using full-field measurements. In: *European Mechanics of Materials Conference – Material and Structural Identification from Full-Field Measurements*, Cachan, France, 13–15 September.

Received November 28, 2006. Accepted April 24, 2007.

Published online July 10, 2007.